



# Warming Yang Promoting Blood Circulation and Diuresis Alleviates Myocardial Damage by Inhibiting Collagen Fiber and Myocardial Fibrosis and Attenuating Mitochondria Signaling Pathway Mediated Apoptosis in Chronic Heart Failure Rats

Yong Chen,<sup>1</sup> Yadan Tu,<sup>1</sup> Lei Du,<sup>1</sup> Ruixue Nan<sup>1</sup> and Yi Ren<sup>1</sup>

<sup>1</sup>Department of Classical Chinese Medicine, Chongqing Hospital of Traditional Chinese Medicine, Chongqing, China

Warming Yang promoting blood circulation and diuresis (WYPBD) has been proven effective in treating some diseases. This study aimed to evaluate therapeutic effect of WYPBD in treating chronic heart failure (CHF). CHF rats were established by intraperitoneally injecting doxorubicin (DOX). Therapeutic effects of WYPBD on cardiac function and hemodynamic parameters of myocardial tissues were analyzed. Collagen fiber production and myocardial fibrosis were evaluated. Transcriptions of *COL1A1* gene, *COL3A1* gene, and *TGFB1* gene were evaluated with RT-PCR. Expression of BNP, AVP, PARP, caspase-3, and Bcl-2 in myocardial tissues were evaluated. TUNEL assay was used to identify apoptosis of cardiomyocytes. WYPBD alleviated degree of myocardial hypertrophy in CHF rats compared to the rats in CHF model group ( $P < 0.05$ ). WYPBD significantly improved cardiac hemodynamics (increased LVEF and LVSF) of CHF rats compared to rats in the CHF model group ( $P < 0.05$ ). WYPBD protected myocardial structure and inhibited collagen fiber production in myocardial tissues of CHF rats. WYPBD markedly decreased myocardial fibrosis mediators (*Col1 $\alpha$* , *Col3 $\alpha$* , *TGF- $\beta$ 1*) transcription in myocardial tissues of CHF rats compared to rats in CHF model group ( $P < 0.05$ ). WYPBD significantly reduced BNP and AVP expression in myocardial tissues of CHF rats compared to rats in the CHF model group ( $P < 0.05$ ). WYPBD markedly reduced the expression of PRAP and caspase-3, and increased Bcl-2 expression in myocardial tissues of CHF rats compared to rats in the CHF model group ( $P < 0.05$ ). In conclusion, WYPBD alleviated CHF myocardial damage by inhibiting collagen fiber and myocardial fibrosis, attenuating apoptosis associated with the mitochondria signaling pathway of cardiomyocytes.

**Keywords:** apoptosis; chronic heart failure (CHF); collagen fiber; myocardial injury; Warming Yang promoting blood circulation and diuresis (WYPBD)

Tohoku J. Exp. Med., 2024 June, 263 (2), 141-150.

doi: 10.1620/tjem.2024.J022

## Introduction

Chronic heart failure (CHF) is caused by various causes, such as changes in the heart structure, dysfunction of ventricular contraction and relaxation, which leads to a decrease in cardiac output and cannot meet body metabolism needs, thus causing a series of diseases such as fatigue, dyspnea, and fluid retention (Waku et al. 2020; Taniguchi et al. 2021). CHF is the last stage of the development of common clinical heart disease. Mortality in patients with severe

heart failure in one year is up to 50%, and the 5-year survival rate is similar to that of malignant tumors (Chioncel et al. 2017). CHF patients generally experience a vicious disorder cycle, including hospitalization, improvement, discharge, rehospitalization (Wang et al. 2019). In China, the prevalence of heart failure among the adult population is approximately 0.9%, indicating that there are about 4 million patients with heart failure in China every year, and 200,000 new cases every year (Wang et al. 2021). At present, ACEI/ARB,  $\beta$  receptor blockers and aldosterone recep-

Received January 8, 2024; revised and accepted March 14, 2024; J-STAGE Advance online publication March 22, 2024

Correspondence: Yi Ren, Department of Classical Chinese Medicine, Chongqing Hospital of Traditional Chinese Medicine, 6 Panxi Qizhi Road, Jiangbei District, Chongqing 400021, China.

e-mail: cqszyzyj@163.com

©2024 Tohoku University Medical Press. This is an open-access article distributed under the terms of the Creative Commons Attribution-NonCommercial-NoDerivatives 4.0 International License (CC-BY-NC-ND 4.0). Anyone may download, reuse, copy, reprint, or distribute the article without modifications or adaptations for non-profit purposes if they cite the original authors and source properly.

<https://creativecommons.org/licenses/by-nc-nd/4.0/>

tor antagonists (MRA) are used in the treatment of chronic heart failure (Greene et al. 2018). Although these drugs can improve the prognosis, the readmission rate and the death rate of patients are still high.

In recent years, research on the pathogenesis of heart failure has undergone important changes. The pathogenesis and treatment of heart failure in Chinese and Western medicine have gradually achieved unity in some aspect. From the perspective of traditional Chinese medicine, in the process of occurrence and development of heart failure, heart *Qi* deficiency is the pathological basis and blood stasis is an inevitable pathological process (Wu et al. 2021). In the early stages of CHF, most patients mainly suffer from a simple *Qi* deficiency, with palpitations, chest tightness, shortness of breath, and mental fatigue (Wang et al. 2019). Therefore, traditional Chinese medicine for invigorating *Qi* and activating blood circulation has been widely used in the treatment of heart failure. Many traditional Chinese medicines have shown efficacy and safety in treating heart failure in both humans and animal models (Li et al. 2013; Wang et al. 2019).

Warming Yang promoting blood circulation and diuresis (WYPBD) is considered a specific traditional Chinese medicine extracted from more than 10 types of herbs (Yuan et al. 2012). WYPBD has been proven to exhibit many pharmacological activities, such as promoting Yang *Qi*, improving blood circulation and facilitating urine excretion, and has been used for mini-nephrotic syndrome (Yuan et al. 2012), endometriosis (Jia et al. 2015) and chronic heart failure (Wang 2011). However, there has been little research focusing on the specific mechanism of efficacy of WYPBD on CHF until now. Therefore, this study aimed to evaluate the efficacy and explore the mechanism of WYPBD for the treatment of CHF in an animal model.

## Materials and Methods

### *Animals, experimental design and CHF modeling*

The specific pathogen-free (SPF) Sprague Dawley male rats (age, 6-8 weeks, weight 200-250 g) (Approval No. SCXK (Chuan) 2020-034) were purchased from Chengdu Kangsheng Biotech Co. Ltd., China.

The experimental design of this study was as follows: After 4 weeks of doxorubicin hydrochloride (DOX)-induced CHF modeling, an echocardiography was conducted to confirm the establishment of CHF rat model. The rats were then administration WYPBD for 4 consecutive weeks once a day. An echocardiography was performed and the heart tissue samples were taken as detection samples for subsequent experiments (such as HE, Masson, QPCR, WB).

For the CHF model, rats ( $n = 30$ ) were injected intraperitoneally with DOX at a dose of 2.5 mg/kg body weight per time for 8 times (2 times/week, continuous injection for 4 weeks), according to a previous study (Wen et al. 2019). DOX injection was not stopped until the total dose of DOX was 20 mg per rat.

### *Ethical statement*

This study was approved by the Ethical Committee of the Chongqing Hospital of Traditional Chinese Medicine, China. All animal processes here were carried out according to the Guide for the Care and Use of Laboratory Animals of the National Institutes of Health. This study has not involved the humans.

### *Preparation of the WYPBD reagent*

The WYPBD was prepared according to the description in a previous study (Huang et al. 2015), which mainly includes the following ingredients: *Radix angelicae sinensis* (Danggui), *Ramulus cinnamomi* (Guizhi), *Radix paeoniae alba* (Baishao), *Herba asari mandshurici* (Xixin), *Radix glycyrrhizae* (honey fried Gancao), *Medulla tetrapanaicis* (Tongcao), *Fructus jujubae* (Dazao), *Radix linderae aggregatae* (Wuyao), *Radix aconiti lateralis preparate* (Fuzi), *Rhizoma zingiberis* (Ganjiang). The above ingredients were boiled and centrifuged at a speed of 2,000 r/min for 10 min and 4,000 r/min for 10 min, to obtain a crude drug at a concentration of 700 mg/ml in liquid. According to the raw drug content marked on the package, the theoretical equivalent dose of rats was obtained by conversion from the Meeh Rubner formula and then dissolved in a suspension with distilled water.

### *Experimental grouping and treatment*

CHF rats were prepared as above and randomly divided into 6 groups with 5 rats in each group, including the CHF model group (intragastrically administering with a dose of 0.2 ml/20 g saline), the CHF+L-WYPBD group (intragastrically administering with a low dose of WYPBD, 0.1 ml/20 g), the CHF+M-WYPBD group (intragastrically administering with a medium dose of WYPBD, 0.2 ml/20 g), the CHF+H-WYPBD group (intragastrically administering with a high dose of WYPBD, 0.4 ml/20 g), the CHF+Cap (intragastrically administering with a dose of captopril (Cap), 0.1 ml/20 g (100 mg/kg)), and the CHF+WYPBD+Cap group (intragastrically administering with a dose of 0.2 ml/20 g WYPBD and 0.1 ml/20 g Cap (100 mg/kg)). While rats in the normal control group (NC,  $n = 5$ ) were administered saline intragastrically at a dose of 0.2 ml/20 g. In this study, the dosage of drugs used by humans was converted into the dosage of experimental animals, which is widely used in traditional Chinese medicine research (Xu et al. 2002).

### *Cardiac function assessment*

Rats in both the CHF model group and the NC group were anesthetized with 7% chloral hydrate, and transthoracic echocardiography was performed with an echocardiography machine equipped with a transducer. In this study, the following parameters were comprehensively evaluated, including the thickness of the interventricular septum in diastole (IVSd), left ventricular end diastolic diameter (LVDD), left ventricular diastolic posterior wall

thickness (LVPWd), interventricular septal thickness at systole (IVSs), left ventricular end systolic diameter (LVDD), left ventricular systolic posterior wall thickness (LVPWs). The following hemodynamic indices were evaluated, including the left ventricular ejection fraction (LVEF), left ventricular fractional shortening (LVFS). Meanwhile, heart weight, heart-to-body weight ratio (heart/weight), ratio of heart weight and diameter of rib (heart/rib diameter).

#### Histological evaluation

Rats were sacrificed by administering an overdose of 7% chloral hydrate and rats' serum and heart tissue were collected and stored at  $-80^{\circ}\text{C}$  to evaluate different biomarkers. Hematoxylin and eosin staining (H&E) and Masson's trichrome staining were conducted to evaluate the morphological characteristics and formation of myocardial fibrosis in heart tissues of rats in each group, according to the description of a previous study (An et al. 2013). Picrosirius red staining was also carried out to evaluate collagen fiber in myocardial tissues, based on a previous report (Kim et al. 2021). Furthermore, immunohistochemical staining was also performed to evaluate myocardial damage biomarkers [brain natriuretic peptide (BNP) and arginine vasopressin (AVP)] and biomarkers associated with apoptosis [poly ADP-ribose polymerase (PARP), caspase-3, and B-cell lymphoma-2 (Bcl-2)], as described by a previously published study (Yang et al. 2014). The dematoxylin and eosin were purchased from Jiancheng Bioengineering Ins. (Cat. No. D006-1-4, Nanjing, China) and Beyotime Biotech Inc. (Shanghai, China). The Masson's trichrome stain kit was purchased from SolarBio (Cat. No. G1343, Beijing, China). Rabbit anti-rat BNP (Cat. No. ab243440), anti-rat VAP (Cat. No. AB213708), anti-rat PARP (Cat. No. ab191217), and anti-rat caspase-3 (Cat. No. ab179517) were purchased from Abcam Biotech (Cambridge, MA, USA), and rabbit anti-rat Bcl-2 antibody (Cat. No. ET1603-11) was purchased from HuaBio. (Guangzhou, China). Horseradish peroxidase (HRP)-labeled goat anti-rabbit IgG (Cat. No. A0208) was purchased from Beyotime Biotech Inc.

#### TUNEL staining

Heart tissues were fixed with 4% paraformaldehyde, embedded with paraffin, and subjected to TUNEL staining

to determine myocardial cell apoptosis. Briefly, the paraffin-fixed heart tissue section was stained using the terminal deoxynucleotidyl transferase (TdT)-mediated dUTP nick end labeling (TUNEL) method, as instructed by the manufacturer (Cat. No. C1091, Beyotime Biotech Inc.)

#### ELISA

Serum levels of BNP and AVP were measured with an ELISA reader (Model: Immulon 4 HBX, Thermo Fisher Scientific, Rockford, IL, USA). All experiments were performed according to the BNP ELISA detection kit protocol (Cat. No. JM-0147R1, Jingmei Bio., Jiangsu, China) and AVP ELISA detection kit (Cat. No. JM-02197R1, Jingmei Bio.).

#### Real-time PCR (RT-PCR)

Total RNA was extracted from the above stored heart tissues with the RNAiso plus RNA extraction kit (Cat. No. 9109Q, Takara Bio., Tokyo, Japan) as a manufacturer protocol. The complementary DNA (cDNA) was synthesized with an Hifair III 1st-strand cDNA synthesis kit (Cat. No. 11139ES10, Yeasen Bio., Shanghai, China), using the above RNAs as template. Then, the RT-PCR assay for amplifying *COL1A1* gene (encoding collagen Ia, *Coll1a*), *COL3A1* gene (encoding collagen IIIa, *Col3a*), and *TGF $\beta$ 1* gene (encoding transforming growth factor- $\beta$ 1, *TGF- $\beta$ 1*) in heart tissues was performed by analyzing with a Hieff UNICON universal blue qPCR Sybr green master mix (Cat. No. 11184ES03, Yeasen Bio.). The primer sequences are listed in Table 1. The relative gene transcription of *Coll1a*, *Col3a*, *TGF- $\beta$ 1* was determined based on calculations of  $2^{-\Delta\Delta C_t}$  with GAPDH as the internal reference.

#### Western blot assay

The western blot assay was performed according to the process of a previous study (Gao et al. 2020), with a few modifications. In summary, total proteins were extracted from heart tissues with pre-cold RIPA buffer (Cat. No. P0013, Beyotime Biotech Inc.). The protein concentration was examined with a BCA protein detection kit (Cat. No. ST-2222, Beyotime Biotech Inc.) as instructed by the manufacturer. Equal amounts of the proteins were loaded to SDS-PAGE and electro-transferred onto the PVDF mem-

Table 1. The primers for the PCR assay.

Genes	Sequences (5'-3')	Length (bp)
<i>Coll1a</i> Forward	CAGACGGGAGTTTCACCTCC	73
<i>Coll1a</i> Reverse	TCTTTGCGGCTGGGGTGG	
<i>GAPDH</i> Forward	GGCAAGTTCAACGGCACAG	142
<i>GAPDH</i> Reverse	CGCCAGTAGACTCCACGACAT	
<i>Col3a</i> Forward	TTCACCCCTCTCTATTTTGGCA	99
<i>Col3a</i> Reverse	CAGATCCCGAGTCGCAGACAC	
<i>TGF</i> Forward	CCAAGGAGACGGAATACAGGG	89
<i>TGF</i> Reverse	CATGAGGAGCAGGAAGGGTC	

branes. Subsequently, the PVDF membranes were incubated with mice anti-rat BNP (Cat. No. ab239510, Abcam Biotech.), rabbit anti-rat AVP (Cat. No. ab213708, Abcam Biotech.), rabbit anti-rat cleaved caspase-3 (Cat. No. AF7022, Affinity Biosciences, Cinchinnati, OH, USA), rabbit anti-rat cleaved PARP (Cat. No. AF7023, Affinity Biosciences), rabbit anti-rat Bcl-2 (Cat. No. ET1702-53, HuaBio.), rabbit anti-rat Bax (Cat. No. ET1603-34, HuaBio.) and rabbit anti-rat GAPDH (Cat. No. EM1101, HuaBio.) antibody at 4°C overnight. The PVDF membranes were then treated with HRP-labeled goat anti-rabbit IgG (Cat. No. A0208, Beyotime Biotech Inc.) or HRP-conjugated goat anti-mouse IgG (Cat. No. A0216, Beyotime Biotech Inc.) at room temperature for 2 h. Finally, protein-antibody bands were detected with an enhanced chemiluminescence (ECL) solution and visualized with the X-ray film. Quantification of the bands was performed with densitometric analyzes using the Tanon-4200 gel imaging system.

### Statistical analysis

Data were expressed as means  $\pm$  SD and analyzed using SPSS 20.0. ANOVA followed by the post hoc Turkey test was used to compare the differences between groups.

The assumptions for normality and homogeneity of variances necessary for means comparisons were analyzed and tested with the Kolmogorov-Smirnov test and the Leven test, respectively (all with normality and homogeneity in this study). A  $P$  value less than 0.05 was considered statistically significant.

## Results

### WYPBD alleviated the degree of myocardial hypertrophy in CHF rats

According to echocardiography findings in this study, the values of LVIDs ( $P = 0.005$ ) were increased significantly, and the values of LVPWd ( $P = 0.004$ ), LVPWs ( $P = 0.036$ ), LVEF ( $P < 0.001$ ), and LVFS ( $P < 0.001$ ) were significantly decreased in CHF rats compared to rats in the NC group (Fig. 1A-C). Therefore, the CHF rat model was successfully established due to the above echocardiography results. WYPBD treatment at all doses increased the LVPWd and LVPWs values of CHF rats compared to those of rats in the CHF model group, however, without significant differences (Fig. 1A, B). Furthermore, WYPBD treatment also improved the inhibitive effects of Cap on myocardial hypertrophy in CHF rats (Fig. 1A, B).

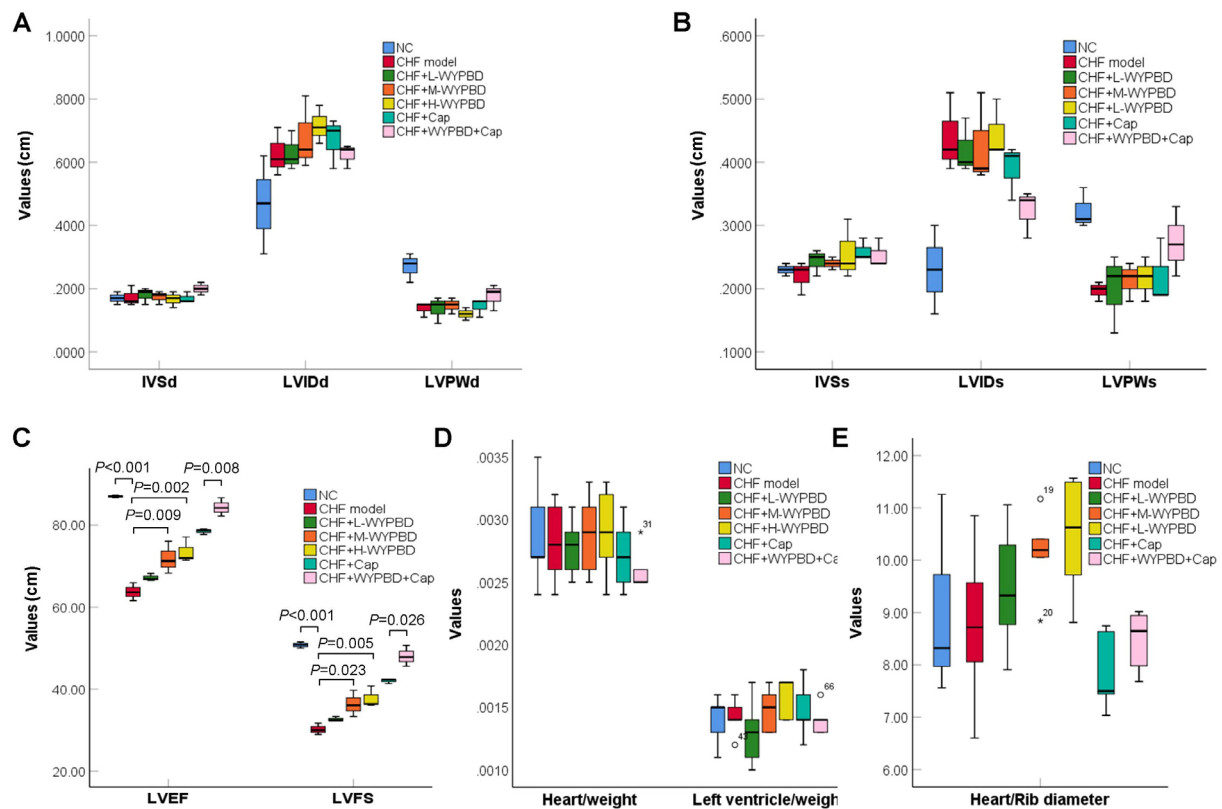


Fig. 1. Effects of WYPBD treatment on the degree of myocardial hypertrophy and cardiac hemodynamics of CHF rats.

A. Comparison of the IVSd, LVIDd, and LVPWd values among different groups. B. Comparison of the IVSs, LVIDs, and LVPWs values among different groups. C. Comparison of the LVEF and LVFS values between different groups. D. Comparison of the heart/weight ratio and the left ventricle/weight ratio among different groups. E. Comparison of the heart/rib diameter ratio among different groups. The  $P$ -values have been labeled in figures to compare the difference between two groups.

### WYPBD improved the cardiac hemodynamics of CHF rats

Due to results of ANOVA, there were significant differences for the LVEF values ( $P < 0.001$ ) and the LVFS values ( $P < 0.001$ ) among rats in all groups (Fig. 1C). The medium dose of WYPBD ( $P = 0.009$ ) and the high dose of WYPBD ( $P = 0.002$ ) significantly increased the LVEF values of CHF rats compared to those of rats in the CHF model group (Fig. 1C). Meanwhile, the LVFS values of CHF rats also increased markedly in rats of both the CHF+M-WYPBD group ( $P = 0.023$ ) and the CHF+H-WYPBD group ( $P = 0.005$ ) compared to rats from the CHF model group (Fig. 1C). Furthermore, WYPBD combining Cap (CHF+WYPBD+Cap group) obviously increased LVEF values ( $P = 0.008$ ) and LVFS values ( $P = 0.026$ ) in CHF rats compared to those of rats in the CHF+Cap group (Fig. 1C).

Furthermore, there were no significant differences for heart/weight ratio ( $P = 0.747$ ), left ventricle/weight ratio ( $P = 0.433$ ) and heart/rib diameter ( $P = 0.320$ ) in rats between different groups (Fig. 1D, E).

### WYPBD protected the myocardial structure and inhibited collagen fiber production

H&E staining showed that the arrangement of the myocardial fibers of CHF rats was disordered and seriously damaged, and some myocardial cells were fragmented (Fig. 2A). While WYPBD treatment at different doses obviously protected the myocardial fibers from damage in the CHF modeling process (Fig. 2A). Masson's staining (Fig. 2B, collagen with blue staining) and Picosirius red staining (Fig. 3C, collagen with red staining) also showed that

WYPBD treatments obviously suppressed collagen fiber production in myocardial tissues of CHF rats. The WYPBD that combined Cap also demonstrated an obvious improvement in myocardial fiber arrangement and suppression of collagen fibers in myocardial tissues of CHF rats compared to that of the CHF+Cap group (Fig. 2A-C).

### WYPBD downregulated the transcriptions of myocardial fibrosis mediator genes in myocardial tissues of CHF rats

In this study, myocardial fibrosis mediators, including *Colla*, *Col3a*, and *TGF- $\beta$ 1*, were identified with an RT-PCR assay. The results showed that there were marked differences for the transcription of *Colla* gene ( $P < 0.001$ ), *Col3a* gene ( $P < 0.001$ ), and *TGF- $\beta$ 1* gene ( $P < 0.001$ ) in myocardial tissues of rats of different groups (Fig. 3A-C). The transcriptions of *Colla* gene ( $P < 0.001$ ), *Col3a* gene ( $P < 0.001$ ), and *TGF- $\beta$ 1* ( $P < 0.001$ ) gene in myocardial tissues of CHF rats were significantly increased compared to those of rats in the NC group. However, WYPBD at low, medium, and high doses markedly decreased the transcriptions of *Colla* gene (Fig. 3A,  $P = 0.001$ ,  $P < 0.001$ ,  $P < 0.001$ ), *Col3a* gene (Fig. 3B, all  $P < 0.001$ ), and *TGF- $\beta$ 1* (Fig. 3C,  $P = 0.005$ ,  $P < 0.001$ ,  $P < 0.001$ ) gene in myocardial tissues of CHF rats compared to those of CHF rats in CHF model group. Furthermore, WYPBD could also strengthen the inhibitive effect of Cap on the transcription of *Colla* gene (Fig. 3A), *Col3a* gene (Fig. 3B), and *TGF- $\beta$ 1* gene (Fig. 3C) in CHF rats compared to those of the CHF+Cap group, however, without significant differences (all  $P > 0.05$ ).

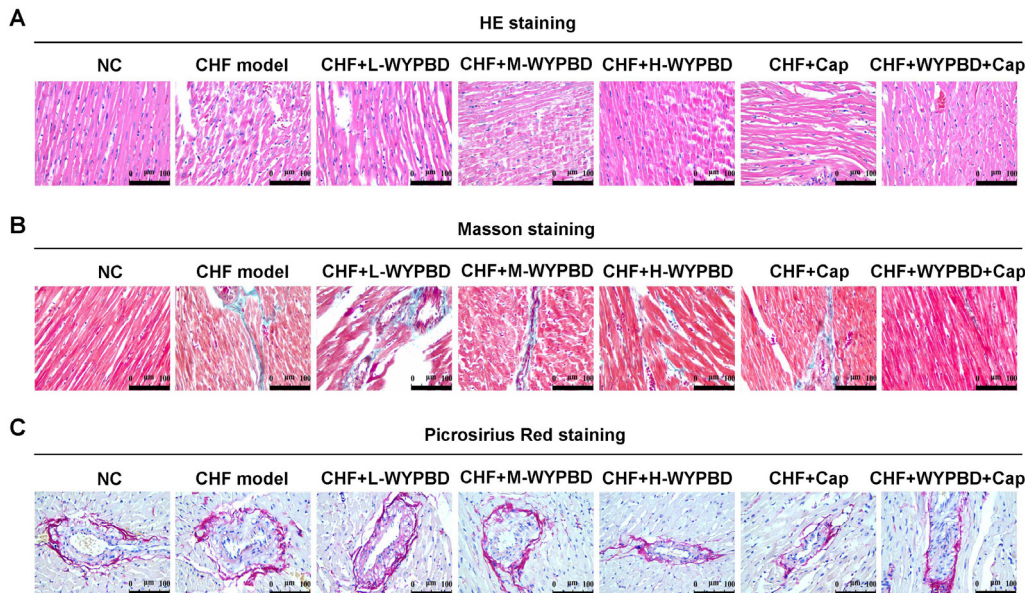


Fig. 2. WYPBD treatment protected the myocardial structure and inhibited the production of collagen fiber in myocardial tissues.

A. H&E staining to indicate the structure of myocardial fibers. B. Masson's staining to demonstrate the production of collagen fibers in myocardial tissues. C. Picosirius red staining for showing the production of collagen fibers in myocardial tissues.

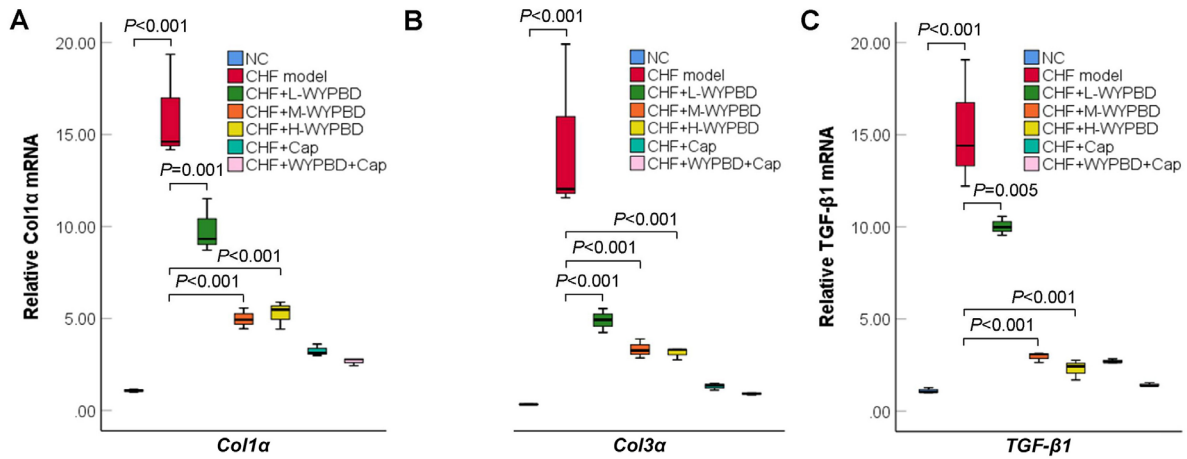


Fig. 3. WYPBD treatment decreased the transcription of myocardial fibrosis mediator genes in the myocardial tissues of CHF rats. A. Transcription of *Col1α* gene identified by RT-PCR assay. B. Transcription of *Col3α* identified by RT-PCR assay. C. Transcription of *TGF-β1* identified with the RT-PCR assay. *P*-values have been labeled in figures to compare the difference between two groups.

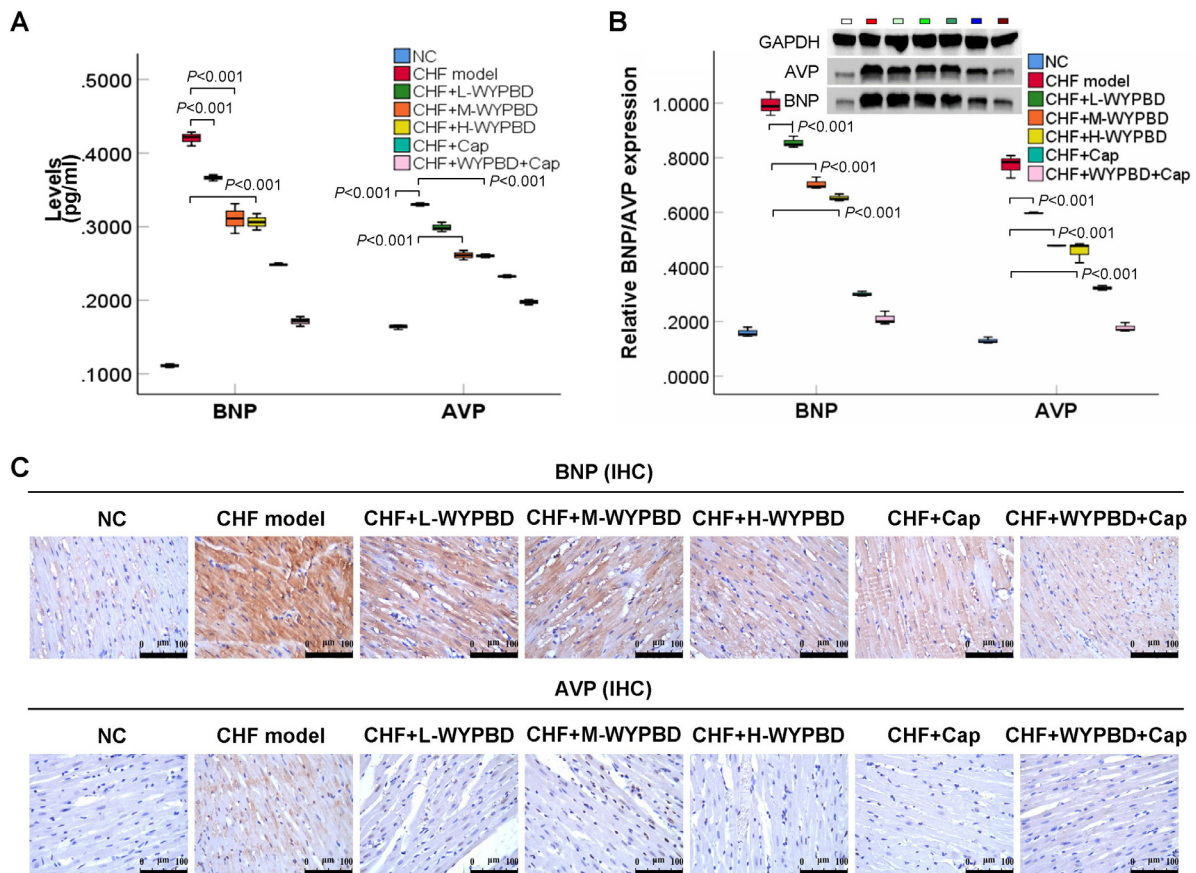


Fig. 4. BNP and AVP gene transcription and expression of CHF rats decreased after WYPBD treatment. A. BNP and AVP levels in serum of CHF rats according to the ELISA assay. B. Expression of BNP and AVP in myocardial tissues of CHF rats according to the Western blot assay. C. Expression of BNP and AVP in myocardial tissues of CHF rats according to the immunohistochemical assay. *P*-values have been labeled in figures to compare the difference between two groups.

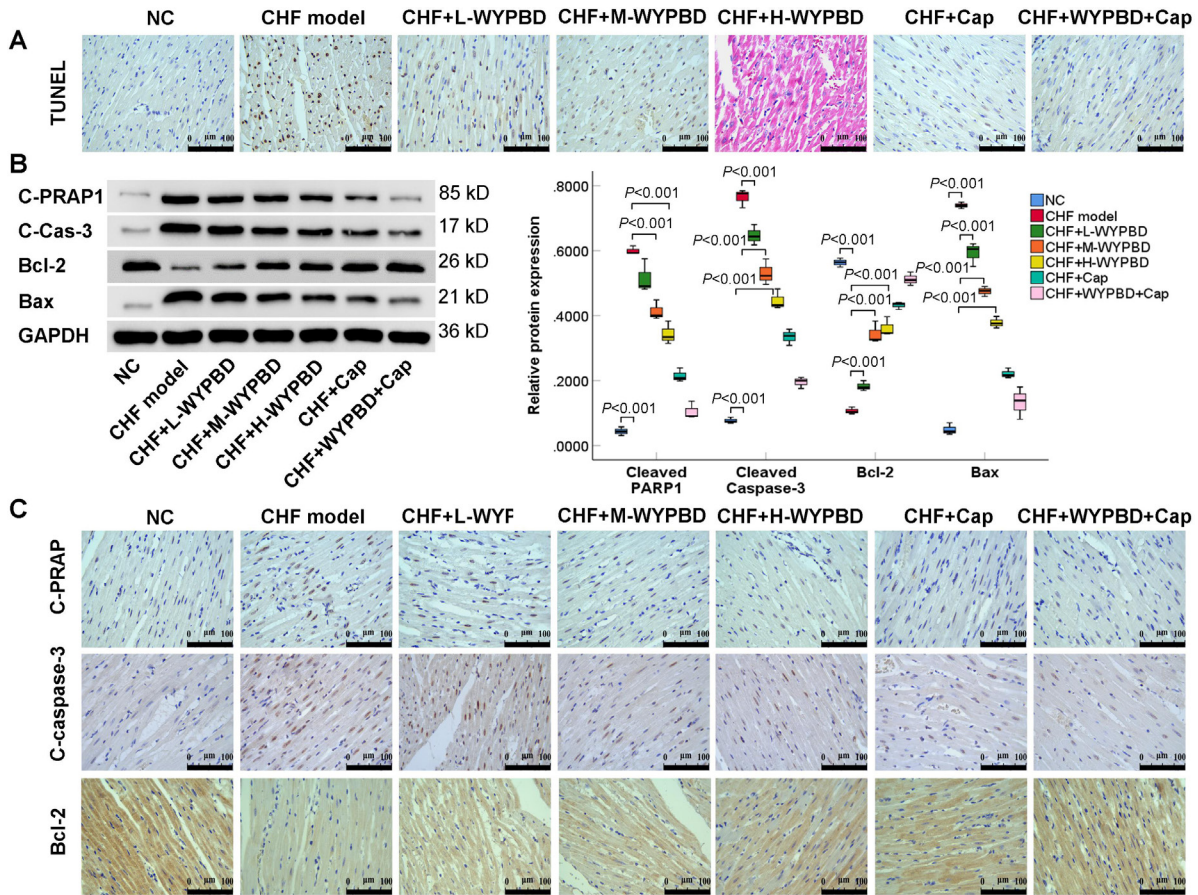


Fig. 5. WYPBD treatment inhibited cardiomyocyte apoptosis in CHF rats.

A. TUNEL assay showing the apoptotic cardiomyocytes (brown staining). B. Western blot assay showing expression of cleaved PRAP (C-PRAP), cleaved caspase-3 (C-caspase-3), Bcl-2, and Bax in myocardial tissues (brown staining). C. Immunohistochemical assay showing the expression of C-PRAP, C-caspase-3, and Bcl-2 in myocardial tissues (brown staining). *P*-values have been labeled in figures to compare the difference between two groups.

#### WYPBD reduced BNP and AVP expression of CHF rats

In this study, the myocardial damage associated biomarkers, BNP and AVp, were evaluated. The transcription of BNP gene and AVP gene in the serum of CHF rats was evaluated with ELISA (Fig. 4A). The expressions of BNP and AVP protein were evaluated using western blot assay (Fig. 4B) and immunohistochemical assay (Fig. 4C). According to the ELISA and statistical analysis, there were marked differences for BNP levels ( $P < 0.001$ ) and AVP levels ( $P < 0.001$ ) in myocardial tissues between different groups. As shown in Fig. 4A, BNP levels (all  $P < 0.001$ ) and AVP levels (all  $P < 0.001$ ) were significantly reduced in myocardial tissues of CHF rats from WYPBD groups compared to CHF rats from the CHF model group. WYPBD also promoted the suppressive effect of Cap (CHF+WYPBD+Cap) on BNP levels ( $P < 0.001$ ) and AVP levels ( $P < 0.001$ ) compared to CHF rats treated with Cap alone (CHF+Cap group) (Fig. 4A). Furthermore, Western blot findings (Fig. 4B) and immunohistochemical results (Fig. 4C) showed that different doses of WYPBD could also decrease BNP expression and AVP expression in myocardial tissues of rats compared to those of CHF rats.

Furthermore, the combination of WYPBD with Cap could also obviously decrease the expressions (levels) of BNP and AVP in the myocardial tissues of CHF rats (CHF+WYPBD+Cap) compared to those of CHF rats from the CHF+Cap group (Fig. 4A-C).

#### WYPBD attenuated mitochondria pathway-associated cardiomyocyte apoptosis

The TUNEL stain showed obvious apoptosis in the myocardial tissues of CHF rats, which were attenuated by different doses of WYPBD (Fig. 5A), therefore, WYPBD could inhibit apoptosis. The biomarkers related to mitochondria pathway apoptosis, Bcl-2, Bax, cleaved PRAP (C-PRAP), and cleaved caspase-3 (C-caspase-3), were determined using both the western blot assay (Fig. 5B) and the immunohistochemical assay (Fig. 5C), respectively. As shown in Fig. 5B, the expression of pro-apoptotic biomarkers (C-PRAP, C-caspase-3, Bax) increased significantly, and the expression of the anti-apoptotic biomarker (Bcl-2) decreased significantly in the myocardial tissues of CHF rats compared to those of the NC group rats (all  $P < 0.001$ ). At the same time, low, medium and high doses of WYPBD

markedly reduced the expression of C-PRAP, C-caspase-3 and Bax, and increased the expression of Bcl-2 in myocardial tissues of CHF rats compared to those of CHF rats of the CHF model group (Fig. 5B, all  $P < 0.001$ ). The immunohistochemical findings showed that the expression of cleaved PARP and cleaved caspase-3 in the myocardial tissues of WYPBD treated CHF rats was obviously decreased, and the expression of Bcl-2 was obviously increased, compared to those of rats in the CHF model group (Fig. 5C). Furthermore, WYPBD could also promote the antiapoptotic effect of Cap in the myocardial tissues of CHF rats (Fig. 5C).

### Discussion

CHF patients are mainly characterized by deterioration in cardiac functions and clinically decreasing athletic tolerance (An et al. 2013). Traditional Chinese medicine has been used to treat patients with CHF accompanied by acute symptoms exacerbating for many years in China (Zhu et al. 2016), therefore, traditional Chinese medicine can serve as an effective and complementary treatment strategy combining with standard treatment strategies. WYPBD, as a form of traditional Chinese medicine, has been long applied to clinical practice in the treatment of different diseases (Zhu et al. 2016) in China and has achieved favorable clinical results. This study demonstrated pharmacodynamics and specific mechanism evidence that WYPBD treatment alleviated the CHF rat model induced by doxorubicin (DOX). According to anti-collagen fiber formation, anti-myocardial damage effects and antiapoptosis functions, these findings suggested that WYPBD may improve myocardial functions by decreasing collagen fiber production and blocking the mitochondrial-associated apoptosis pathway in the myocardial tissues of CHF rats. To our knowledge, this is the first study investigating the protective effects of WYPBD on DOX-induced CHF.

In this study, DOX-induced CHF rat model was successfully established via intraperitoneally injected with DOX at a dose of 2.5 mg/kg body weight per time for 8 times (Wen et al. 2019). The potential mechanism for the DOX-induced cardiotoxicity seems to be multifactorial. However, some previous studies (Cui et al. 2017; Wang et al. 2019) proved that the DOX-induced CHF rat model demonstrated obvious cardiotoxic effects of DOX, such as cardiomyocyte apoptosis, dysmodulation of metabolites, cardiac energy homeostasis, and myocardial inflammation. Based on echocardiography findings of increased LVIDs values and decreased LVPWd, LVPWs, LVEF and LVFS values in CHF rats in the present study, suggesting that the CHF rat model was successfully established. The echocardiography diagnosis of CHF rats also showed that the left ventricular ejection fraction was less than 50%, indicating the successful modeling of heart failure. These findings are similar to those experimental heart failure models previously established (Bai et al. 2017; Wu et al. 2019; Sun et al. 2021; Wei et al. 2022; Xu et al. 2022; Suto et al. 2023). Furthermore, according to the design plan of this study, an

echocardiogram test was performed after the construction of the CHF model, with the aim of screening the successfully modeled rats. After completion of WYPBD treatment, this study conducted another echocardiography test to observe the treatment status of the medication to ensure that CHF model is effective during drug therapy process. Furthermore, the CHF model rats were prone to death during the modeling process. Anesthesia is required for each echocardiography, and excessive time point echocardiography detection may lead to a higher number of rat deaths, making it impossible to carry out subsequent experiments.

WYPBD treatment at all doses improved the LVPWd and LVPWs values of CHF rats compared to those of rats in the CHF model group. WYPBD treatment also improved the inhibitive effects of Cap on myocardial hypertrophy in CHF rats. These results suggest that WYPBD could obviously alleviate myocardial hypertrophy during the CHF modeling process. Meanwhile, the values of LVEF and LVFS increased significantly in CHF rats treated with WYPBD compared to those of rats in the CHF model group, suggesting that WYPBD could improve the cardiac hemodynamics of CHF rats.

Myocardial dysfunction must be caused by the injury or damage to the myocardium (Yu et al. 2018), therefore, we determined myocardial structures and collagen fiber formation in the myocardial tissues of CHF rats. H&E staining showed the disordered arrangement of myocardial fibers and seriously damaged myocardial tissues in CHF rats, while WYPBD obviously protected against these damages. Masson's and Picrosirius red staining showed that WYPBD obviously suppressed collagen fiber production in the myocardial tissues of CHF rats. Meanwhile, WYPBD in combination with Cap obviously improved myocardial fiber arrangement and suppressed collagen fibers in the myocardial tissues of CHF rats. Furthermore, the gene transcriptions of the mediators of myocardial fibrosis in the myocardial tissues of CHF rats (Ma et al. 2019), including *Colla*, *Col3a*, and *TGF- $\beta$ 1*, were significantly decreased by WYPBD administration. These findings suggest that WYPBD could protect myocardial structure, inhibit collagen fiber production, and suppress myocardial fibrosis.

BNP is released mainly from the left ventricle as a response to increased filling pressure and injury (Kjaer et al. 2004). Increased AVP levels in CHF patients were closely correlated with long-term outcomes, such as death (Lanfeer et al. 2013). Therefore, both BNP and AVP were used as biomarkers to evaluate myocardial damage. The results of the ELISA, Western blot, and immunohistochemical assays demonstrated that BNP levels (or expressions) and AVP levels (or expressions) were significantly reduced in serum or myocardial tissues of CHF rats from the WYPBD groups compared to the CHF model group. Therefore, WYPBD alleviated myocardial damage by reducing BNP and AVP expression in the serum or myocardial tissues of CHF rats.

The infarcted wall thinning causes scar formation,

while the noninfarcted myocardium causes myocardial hypertrophy in response to increased growth factors and stress (Gao et al. 2020). Cardiomyocyte apoptosis usually occurs during the development of myocardial hypertrophy and induces heart failure (Whelan et al. 2010). Here, the TUNEL staining result indicated that WYPBD obviously attenuated cardiomyocyte apoptosis. Therefore, to verify that WYPBD triggered an alleviated degree of myocardial hypertrophy, biomarkers associated with apoptosis (You et al. 2013), including cleaved PRAP, cleaved caspase-3, Bax and Bcl-2, were detected in myocardial tissues of CHF rats. Our findings showed that WYPBD significantly decreased the expression of the pro-apoptotic biomarkers (cleaved PRAP, cleaved caspase-3, Bax) and markedly increased the expression of the anti-apoptotic biomarker (Bcl-2) in the myocardial tissues of CHF rats. Meanwhile, WYPBD also promoted the antiapoptotic effect of Cap on the myocardial tissues of CHF rats. According to a previous study, Bcl-2, Bax, cleaved caspase-3 and cleaved PRAP belong to the mitochondrial associated apoptosis pathway, therefore, WYPBD attenuated cardiomyocyte apoptosis by activating mitochondrial associated signaling. Furthermore, inflammation as well as the apoptosis could also contribute to the DOX-induced cardiotoxicity, therefore, it is essential to evaluate the inflammation of the myocardial tissues of CHF rats.

This study also has some limitations. First, the sample size of the CHF rat model was relatively small. In the next study, we would involve more rats to further confirm the associated findings and conclusions. Second, the detection of LVEF and LVFS did not adequately represent the hemodynamics, and we would directly evaluate the therapeutic effect of WYPBD on hemodynamic parameters by catheterization. Third, we have not analyzed the specific reason that WYPBD selectively affected the LV hypertrophy at sites within LV (posterior wall) in this study. Fourth, the difference in fibrosis and/or gene expressions between IVS and PW in DOX-induced rat heart failure model has not been clarified. We would explore the specific mechanism for the effect of WYPBD on LV hypertrophy and determine fibrosis and gene expression in DOX-induced rat heart failure model. Fifth, this study only investigated effect of WYPBD in CHF rat model, but not in cultured cells. We would conduct the cultured cell-based assays to reveal the molecular mechanism underlying effect of WYPBD treatment. Sixth, although biomarker expressions of mitochondria pathway mediated apoptosis were evaluated, this study has not shown evidence of mitochondrial dysfunction. We would identify mitochondrial dysfunction and further confirm conclusion of this study. Seventh, this study investigated effects of WYPBD and captopril alone and in combination on CHF, however, the mechanism of their combined effects has not been clearly discussed.

In conclusion, this study demonstrated that WYPBD effectively alleviated myocardial damage by inhibiting collagen fiber production and myocardial fibrosis and by atten-

uating apoptosis mediated by the mitochondria signaling pathway of cardiomyocytes in CHF rat model. These findings may provide evidence for the potential therapeutic effects of WYPBD on CHF in the clinic.

### Acknowledgments

This study was granted by the Chongqing Education Commission Science and Technology Research Program (Grant No. KJZD-K202215103) and Chongqing Natural Science Foundation (Grant No. CSTB2022NSCQ-MSXO978).

### Conflict of Interest

The authors declare no conflict of interest.

### References

- An, Z., Yang, G., He, Y.Q., Dong, N., Ge, L.L., Li, S.M. & Zhang, W.Q. (2013) Atorvastatin reduces myocardial fibrosis in a rat model with post-myocardial infarction heart failure by increasing the matrix metalloproteinase-2/tissue matrix metalloproteinase inhibitor-2 ratio. *Chin. Med. J. (Engl.)*, **126**, 2149-2156.
- Bai, Y., Chen, Q., Sun, Y.P., Wang, X., Lv, L., Zhang, L.P., Liu, J.S., Zhao, S. & Wang, X.L. (2017) Sulforaphane protection against the development of doxorubicin-induced chronic heart failure is associated with Nrf2 Upregulation. *Cardiovasc. Ther.*, **35**, doi: 10.1111/1755-5922.12277. [Epub ahead of print].
- Chioncel, O., Lainscak, M., Seferovic, P.M., Anker, S.D., Crespo-Leiro, M.G., Harjola, V.P., Parissis, J., Laroche, C., Piepoli, M.F., Fonseca, C., Mebazaa, A., Lund, L., Ambrosio, G.A., Coats, A.J., Ferrari, R., et al. (2017) Epidemiology and one-year outcomes in patients with chronic heart failure and preserved, mid-range and reduced ejection fraction: an analysis of the ESC Heart Failure Long-Term Registry. *Eur. J. Heart Fail.*, **19**, 1574-1585.
- Cui, L., Guo, J., Zhang, Q., Yin, J., Li, J., Zhou, W., Zhang, T., Yuan, H., Zhao, J., Zhang, L., Carmichael, P.L. & Peng, S. (2017) Erythropoietin activates SIRT1 to protect human cardiomyocytes against doxorubicin-induced mitochondrial dysfunction and toxicity. *Toxicol. Lett.*, **275**, 28-38.
- Gao, G., Chen, W., Yan, M., Liu, J., Luo, H., Wang, C. & Yang, P. (2020) Rapamycin regulates the balance between cardiomyocyte apoptosis and autophagy in chronic heart failure by inhibiting mTOR signaling. *Int. J. Mol. Med.*, **45**, 195-209.
- Greene, S.J., Butler, J., Albert, N.M., DeVore, A.D., Sharma, P.P., Duffy, C.I., Hill, C.L., McCague, K., Mi, X., Patterson, J.H., Spertus, J.A., Thomas, L., Williams, F.B., Hernandez, A.F. & Fonarow, G.C. (2018) Medical therapy for heart failure with reduced ejection fraction: the CHAMP-HF registry. *J. Am. Coll. Cardiol.*, **72**, 351-366.
- Huang, Y., Shen, L., Cai, A. & Xiao, J. (2015) Effect of warming Yang and removing blood stasis method on matrix metalloproteinases / tissue inhibitor metalloproteinases levels secreted by cultured endometrial cells from patients with endometriosis. *J. Tradit. Chin. Med.*, **35**, 571-576.
- Jia, Y.B., Du, H.L., Gao, X., Bian, W.H., Lin, X.H., Ban, G.G. & Tian, Q.H. (2015) Effects of Bushen Wenyang Huayu Recipe on expressions of HIF-1 $\alpha$ , PHD2, and VHL in endometriosis rats with Shen yang deficiency blood stasis syndrome. *Zhongguo Zhong Xi Yi Jie He Za Zhi*, **35**, 1210-1217.
- Kim, G.J., Jung, H., Lee, E. & Chung, S.W. (2021) Histone deacetylase inhibitor, mocetinostat, regulates cardiac remodeling and renin-angiotensin system activity in rats with transverse aortic constriction-induced pressure overload cardiac hypertrophy. *Rev. Cardiovasc. Med.*, **22**, 1037-1045.

- Kjaer, A., Appel, J., Hildebrandt, P. & Petersen, C.L. (2004) Basal and exercise-induced neuroendocrine activation in patients with heart failure and in normal subjects. *Eur. J. Heart Fail.*, **6**, 29-39.
- Lanfear, D.E., Sabbah, H.N., Goldsmith, S.R., Greene, S.J., Ambrosy, A.P., Fought, A.J., Kwasny, M.J., Swedberg, K., Yancy, C.W., Konstam, M.A., Maggioni, A.P., Zannad, F. & Gheorghiade, M.; EVEREST trial investigators (2013) Association of arginine vasopressin levels with outcomes and the effect of V2 blockade in patients hospitalized for heart failure with reduced ejection fraction: insights from the EVEREST trial. *Circ. Heart Fail.*, **6**, 47-52.
- Li, X., Zhang, J., Huang, J., Ma, A., Yang, J., Li, W., Wu, Z., Yao, C., Zhang, Y., Yao, W., Zhang, B. & Gao, R.; Efficacy and Safety of Qili Qiangxin Capsules for Chronic Heart Failure Study Group (2013) A multicenter, randomized, double-blind, parallel-group, placebo-controlled study of the effects of qili qiangxin capsules in patients with chronic heart failure. *J. Am. Coll. Cardiol.*, **62**, 1065-1072.
- Ma, C., Fu, Z., Guo, H., Wei, H., Zhao, X. & Li, Y. (2019) The effects of Radix Angelica Sinensis and Radix Hedysari ultra-filtration extract on X-irradiation-induced myocardial fibrosis in rats. *Biomed. Pharmacother.*, **112**, 108596.
- Sun, X., Song, Y., Xie, Y., Han, J., Chen, F., Sun, Y., Sui, B. & Jiang, D. (2021) Shenlijia attenuates doxorubicin-induced chronic heart failure by inhibiting cardiac fibrosis. *Evid. Based Complement. Alternat. Med.*, **2021**, 6659676.
- Suto, H., Suto, M., Inui, Y. & Okamura, A. (2023) Late-onset doxorubicin-induced congestive heart failure in an elderly cancer survivor: a case report. *Front. Cardiovasc. Med.*, **10**, 1124276.
- Taniguchi, C., Seto, N. & Shimizu, Y. (2021) Outpatient nursing support for self-monitoring in patients with chronic heart failure. *PLoS One*, **16**, e0254019.
- Waku, R., Tokoi, S., Toyoda, S., Kitahara, K., Naganuma, J., Yazawa, H., Sakuma, M., Abe, S., Nakajima, T. & Inoue, T. (2020) Flow-mediated vasodilation and reactive hyperemia index in heart failure with reduced or preserved ejection fraction. *Tohoku J. Exp. Med.*, **252**, 85-93.
- Wang, S.B. (2011) Clinical observation of treating chronic heart failure by Yiqi Wenyang blood and water. *Clin. J. Chin. Med.*, **2**, 53-54.
- Wang, X., Zhao, Z., Mao, J., Du, T., Chen, Y., Xu, H., Liu, N., Wang, X., Wu, J., Li, R., Xu, Y., Zhao, Y., Wang, L., He, J., Zhang, J., et al. (2019) Randomized, double-blinded, multicenter, placebo-controlled trial of Shenfu injection for treatment of patients with chronic heart failure during the acute phase of symptom aggravation (yang and qi deficiency syndrome). *Evid. Based Complement. Alternat. Med.*, **2019**, 9297163.
- Wang, Z.R., Zhou, J.W., Liu, X.P., Cai, G.J., Zhang, Q.H. & Mao, J.F. (2021) Effects of WeChat platform-based health management on health and self-management effectiveness of patients with severe chronic heart failure. *World J. Clin. Cases*, **9**, 10576-10584.
- Wei, W., Qingling, L.I., Qiang, M.A., Ran, X., Bing, G., Yi, W. & Jing, W. (2022) Effects of moxibustion at bilateral Feishu (BL13) and Xinshu (BL15) combined with benazepril on myocardial cells apoptosis index and apoptosis-related proteins cytochrome c and apoptosis-inducing factor in rats with chronic heart failure. *J. Tradit. Chin. Med.*, **42**, 227-233.
- Wen, J., Zhang, L., Liu, H., Wang, J., Li, J., Yang, Y., Wang, Y., Cai, H., Li, R. & Zhao, Y. (2019) Salsolinol attenuates doxorubicin-induced chronic heart failure in rats and improves mitochondrial function in H9c2 cardiomyocytes. *Front. Pharmacol.*, **10**, 1135.
- Whelan, R.S., Kaplinskiy, V. & Kitsis, R.N. (2010) Cell death in the pathogenesis of heart disease: mechanisms and significance. *Annu. Rev. Physiol.*, **72**, 19-44.
- Wu, Y.J., Wang, Z.B., Li, Y., Wang, D.P., Miao, L., Ren, J.G., Pan, Y.H. & Liu, J.X. (2021) Chronic heart failure due to Qi deficiency and blood stasis and intervention mechanism of compound renshen buqi granules: a proteomics-based study. *Zhongguo Zhong Yao Za Zhi*, **46**, 5052-5063.
- Wu, Z., Zhao, X., Miyamoto, A., Zhao, S., Liu, C., Zheng, W. & Wang, H. (2019) Effects of steroidal saponins extract from *Ophiopogon japonicus* root ameliorates doxorubicin-induced chronic heart failure by inhibiting oxidative stress and inflammatory response. *Pharm. Biol.*, **57**, 176-183.
- Xu, S.Y., Bian, R.L. & Chen, X. (2002) *Pharmacological Experimental Methodology*, 2nd ed., People's Health Publishing House, Beijing, China, pp. 1052-1053.
- Xu, Z., Hu, Z., Xu, H., Zhang, L., Li, L., Wang, Y., Zhu, Y., Yang, L. & Hu, D. (2022) Liquiritigenin alleviates doxorubicin-induced chronic heart failure via promoting ARHGAP18 and suppressing RhoA/ROCK1 pathway. *Exp. Cell Res.*, **411**, 113008.
- Yang, C., Liu, Z., Liu, K. & Yang, P. (2014) Mechanisms of Ghrelin anti-heart failure: inhibition of Ang II-induced cardiomyocyte apoptosis by down-regulating AT1R expression. *PLoS One*, **9**, e85785.
- You, O.H., Kim, S.H., Kim, B., Sohn, E.J., Lee, H.J., Shim, B.S., Yun, M., Kwon, B.M. & Kim, S.H. (2013) Ginkgetin induces apoptosis via activation of caspase and inhibition of survival genes in PC-3 prostate cancer cells. *Bioorg. Med. Chem. Lett.*, **23**, 2692-2695.
- Yu, S.Y., Dong, B., Fang, Z.F., Hu, X.Q., Tang, L. & Zhou, S.H. (2018) Knockdown of lncRNA AK139328 alleviates myocardial ischaemia/reperfusion injury in diabetic mice via modulating miR-204-3p and inhibiting autophagy. *J. Cell. Mol. Med.*, **22**, 4886-4898.
- Yuan, J., Lu, Y.F. & Hang, Q.X. (2012) Effect of formula of warming Yang, promoting blood circulation and diuresis on expression of nephrin in rat with ariamycin-induced nephropathy. *J. Clin. Nephrol.*, **12**, 281-285.
- Zhu, L., Chen, Q.H. & Xu, W. (2016) Clinical observation of 40 cases of acute heart failure with the therapy of SFI. *Chengdu University of Traditional Chinese Medicine*, **9**, 190-192.